

# A NURBS-BASED APPROACH FOR SHAPE AND TOPOLOGY OPTIMIZATION OF FLOW DOMAINS

JAKOB MUNZ<sup>1</sup> AND MICHAEL SCHÄFER<sup>1</sup>

<sup>1</sup> Institute of Numerical Methods in Mechanical Engineering,  
Technische Universität Darmstadt  
Dolivostraße 15, 64293 Darmstadt, Germany  
e-mail: munz@fmb.tu-darmstadt.de, web: <http://www.fmb.tu-darmstadt.de>

**Key words:** Topology Optimization, Brinkman Penalization Method, NURBS (Non-Uniform Rational B-Splines), Finite Volume Method, Navier-Stokes Equations.

**Abstract.** In the present work a NURBS-based framework for shape and topology optimization is presented. The methodology uses fixed grids with immersed boundaries based on a Brinkman penalization method. Compared to other available approaches for topology optimization the number of design variables is reduced and a mathematical description of the solid boundaries is given by NURBS. Two test cases are used to investigate the presented method. The first one compares the proposed method with a traditional shape optimization approach using body-fitted grids. The second one proves the capability of the method for topological changes of the flow domain during the optimization process.

## 1 INTRODUCTION

Shape and topology optimization are important engineering tools for generating optimal fluid flow domains during a development process. For shape optimization usually body-fitted grids are used. However, for complex geometries or large deformations of the grid during the optimization process the grid generation is a challenging problem. This becomes even more difficult for topology optimization problems where the topology of the flow domain may change. To overcome these issues a variety of methods have been developed which use a fixed grid. For a general overview of these methods the reader is referred to [1, 2]. Some of the issues all these methods have in common is a high number of design variables and a slow convergence of the optimization process [3]. To reduce the number of design variables and to ensure smooth, mathematically described interfaces the present work utilizes non-uniform rational basis splines (NURBS) for the solid-fluid interface representation. The control points of the NURBS are used as design variables and by that it is possible to generate complex shapes with a small number of design variables. To model the solid part of the flow domain a Brinkman penalization method [4] is used. An additional advantage of using NURBS is that they are commonly used in computer-aided design (CAD) what makes it is easy to transfer the design of the optimal solution to a CAD system for further post-processing.

## 2 BRINKMAN PENALIZATION METHOD

For the computations in this paper the penalized incompressible Navier-Stokes equations

$$\nabla \cdot \mathbf{v} = 0, \quad (1)$$

$$\rho \left( \frac{\partial \mathbf{v}}{\partial t} + (\mathbf{v} \cdot \nabla) \mathbf{v} \right) = -\nabla p + \mu \Delta \mathbf{v} + \mathbf{f} - \alpha \mathbf{v} \quad (2)$$

are used, where  $\mathbf{v}$  is the flow velocity vector,  $p$  is the pressure,  $t$  is the time,  $\rho$  is the density,  $\mu$  is the dynamic viscosity and  $\mathbf{f}$  are external body forces. The term  $\alpha \mathbf{v}$  is the so called Brinkman penalization term with the Brinkman penalization parameter  $\alpha$ . In fluid regions, this parameter is set to zero and the Brinkman term vanishes which leads to the original Navier-Stokes equations. To ensure the zero-velocity condition in the solid parts, a high value of  $\alpha$  is chosen which causes the velocity to tend towards zero. Referring to [5] where a value of  $\alpha_{max} > 10^4$  is considered as sufficient, the maximum value of  $\alpha$  is set to  $\alpha_{max} = 10^5$  in the present paper.

## 3 NURBS-BASED FRAMEWORK

The proposed methodology uses non-uniform rational basis splines (NURBS) for the geometric representation of the immersed solid boundaries. For the sake of simplicity this paper only considers the two-dimensional case. However, the extension of the proposed method for three-dimensional problems is straight forward. A two-dimensional NURBS curve is defined as

$$\mathbf{C}(u) = \sum_{i=0}^n R_{i,p}(u) \mathbf{P}_i \quad (3)$$

with the independent variable  $u \in [a, b]$ ,  $n+1$  control points  $\mathbf{P}_i$  and the rational basis functions

$$R_{i,p}(u) = \frac{N_{i,p}(u) w_i}{\sum_{j=0}^n N_{j,p}(u) w_j}, \quad (4)$$

where  $w_i$  are the weights and  $N_{i,p}$  are the B-spline basis functions of degree  $p$  defined on a knot vector  $U$ . This vector can be defined in several ways depending of the desired type of the NURBS curve. In the present paper two types are considered. In case of open curves a clamped, uniform knot vector

$$U = \left\{ \underbrace{a, \dots, a}_{p+1}, u_{p+1}, \dots, u_{n-p}, \underbrace{b, \dots, b}_{p+1} \right\} \quad (5)$$

is used. For this kind of vector the first and last knot values are repeated  $p+1$  times. In case of closed curves unclamped, uniform knot vectors

$$U = \{0, \dots, n+1\} \quad (6)$$

are used. For the definition of the basis functions and more details about NURBS in general the reader is referred to [6, 7]. In order to use the NURBS for the optimization

process several parameters can be defined as variable and therefore can be used as design variables. However, in this paper only the coordinates of the control points  $\mathbf{P}_i$  are used for this. The weights are always set to one and the knot vector will be defined depending on the respective test case.

In the following, each step of the optimization process is explained briefly. First, the optimization boundaries have to be described by NURBS curves. In simple cases, this can be done manually by positioning the control points, setting the weights and defining the knot vectors. For more complex geometries immersed into the flow domain this could also be done by common CAD systems which mostly are using NURBS for their geometry description. The coordinates of the control points of these NURBS then have to be coupled to the design variables of the optimization problem. As mentioned before, also other parameters of the NURBS curve could be coupled to design variables which would give even more control over the shape of the curves. However, to keep the number of design variables small only the control points are considered in the present paper. In the next step, the values of the Brinkman penalization parameters  $\alpha$  have to be determined. For this purpose, the proportion of fluid to solid has to be calculated in each control volume which can be done by means of a polygon clipping algorithm. In the present paper the Sutherland-Hodgman algorithm [8] is used. This algorithm clips any convex polygon against any other convex or concave polygon. For the methodology proposed the NURBS curve is clipped against each control volume. In order to do this, the NURBS curve first has to be discretized to create a polygon which then can be clipped by the Sutherland-Hodgman algorithm. Figure 1 shows the procedure for a concave polygon clipped against a quadrilateral control volume where the polygon is clipped successively against all four sides of the control volume starting with the left side. The area of the clipped polygon is

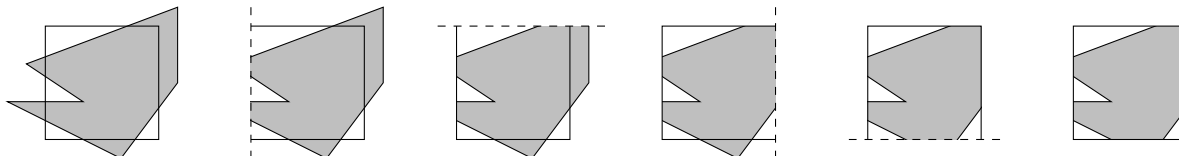


**Figure 1:** Procedure of the Sutherland-Hodgman polygon clipping algorithm

then set in ratio to the total area of the control volume. The resulting volume fraction is used to calculate the corresponding Brinkman penalization parameter. For all control volumes outside the area enclosed by the polygon respectively the NURBS curve the Brinkman penalization parameter is set to  $\alpha = 0$  and for all control volumes inside this area the parameter is set to  $\alpha = 10^5$ . For the control volumes getting cut by the NURBS curve the Brinkman penalization parameter is set to  $0 < \alpha < 10^5$  depending on the volume fraction. By this the immersed boundary gets slightly blurred which is necessary to have a continuous objective function respectively being able to compute a gradient. The last step is solving the fluid flow problem to determine the objective function and all constraints of the optimization problem. For the present paper the block-structured finite volume based solver FASTEST-3D [9] is used for all computations. If the value of the

objective function satisfies the stopping criteria of the optimization method the process is stopped. Otherwise the design variables are adjusted and the process starts over again.

What should be mentioned at this point is that the calculation of the volume fractions by using the Sutherland-Hodgman algorithm can take a not negligible amount of time if the number of control volumes increases since every section of the polygon is checked for intersection with every control volume side. Therefore, the number of sections of the discretized NURBS curve should be as small as possible while still being able to represent the desired immersed boundary. It should also be mentioned that for the proposed methodology no new boundaries can emerge anywhere in the flow domain. Only existing boundaries can merge or vanish. This kind of topology optimization is often referred to in the literature as generalized shape optimization.

## 4 NUMERICAL EXAMPLES

To investigate the presented methodology it is first compared to a NURBS-based shape optimization method which uses body-fitted grids. Then, the capability for topological changes during the optimization process is shown with a second test case. For both test cases the globally convergent version of the method of moving asymptotes (GCMMA) [10] is used, which is a common optimization method in the field of topology optimization. The gradient of the objective function and the constraints required for this algorithm is approximated by forward difference. The tolerance for the stopping criteria is set to  $10^{-5}$  for the relative change of the objective function and the design variables as well as the constraint violation.

### 4.1 Shape optimization of a diffuser

In this test case a shape optimization of a diffuser is performed to reach a specific value of the pressure at its outlet. The results of the proposed methodology are compared with the results of a shape optimization method using a body-fitted grid as shown in [11]. The geometry of the diffuser is depicted in Figure 2. The optimization boundary is described

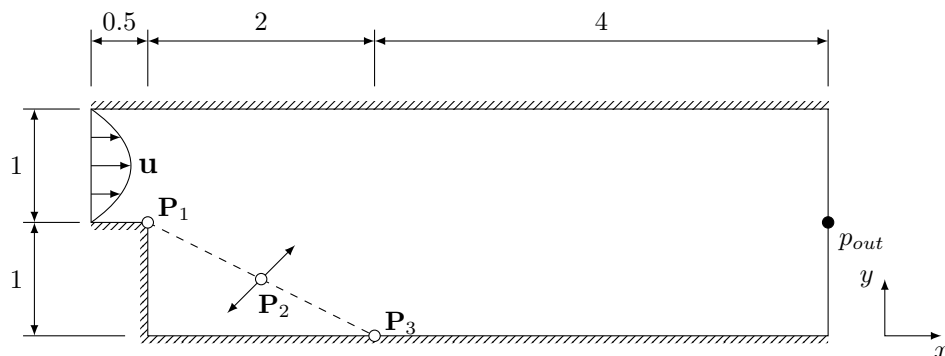


**Figure 2:** Flow domain of the diffuser test case with inlet and outlet boundary conditions and position of the design variable

by an open NURBS curve represented by the dashed line. It is defined by the control

points

$$\mathbf{P}_1 = \begin{pmatrix} 0.5 \\ 1.0 \end{pmatrix}, \quad \mathbf{P}_2 = \begin{pmatrix} 1.5 \\ 0.5 \end{pmatrix}, \quad \mathbf{P}_3 = \begin{pmatrix} 2.5 \\ 0.0 \end{pmatrix} \quad (7)$$

and the knot vector  $U = \{0, 0, 0, 1, 1, 1\}$ . All weights are set to one. Every control volume below this curve is treated as solid. According to [11] the inflow is described by a parabolic velocity profile with a Reynolds number of  $Re = 1$  based on the inlet channel height. The pressure reference point is placed so that the pressure at the inlet is zero and by that the pressure at  $p_{out}$  corresponds to the pressure loss in the diffuser. The objective is to achieve a static pressure of  $-13.5$  Pa at the point  $p_{out}$  by deforming the geometry of the diffuser. To achieve the desired value the optimization problem is defined as

$$\begin{aligned} \min_a \quad & J = (p_{out} + 13.5 \text{ Pa})^2, \\ \text{s. t.} \quad & -0.2 \leq a \leq 0.5. \end{aligned} \quad (8)$$

The design variable  $a$  will move the control point  $\mathbf{P}_2$  and by that deform the NURBS curve with

$$\mathbf{P}_2 = \begin{pmatrix} 1.5 \\ 0.5 \end{pmatrix} - a \cdot \begin{pmatrix} 1 \\ 1 \end{pmatrix}. \quad (9)$$

The initial value of the design variable is set to  $a = -0.2$ , which means that the control point is moved upwards. The results for the optimizations are shown in Figure 3. It can be

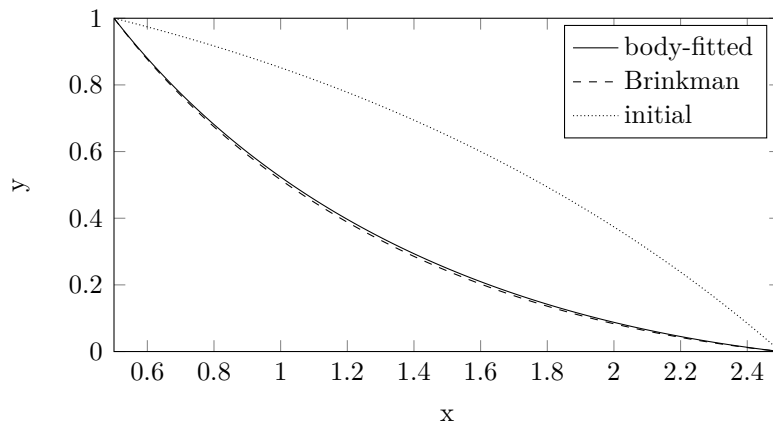


**Figure 3:** Comparison of the resulting NURBS curves for the body-fitted grid and the Brinkman penalization method including the initial curve

seen that the final NURBS curves for the body-fitted grid and the Brinkman penalization method are almost identical. The value of the design variable for the body-fitted grid is  $a = 0.343$  and the value of the Brinkman penalization method is  $a = 0.355$ . For both approaches the pressure at the outlet matches the desired value of  $p_{out} = -13.5$  Pa. Thus, the proposed methodology is a reasonable alternative to classical shape optimization approaches. However, it has to be mentioned that an advantage of body-fitted shape optimization is the simple consideration of turbulent flows. The requirement to have

a very fine grid resolution at the boundaries can be easily fulfilled in any optimization iteration since the grid moves with the boundaries. For approaches with a fixed grid like the Brinkman penalization method the grid doesn't move with the boundary and therefore a prior grid refinement isn't possible. However, to overcome this problem several methods for an adaptive mesh refinement exist which can be used for immersed boundary methods like the one proposed.

## 4.2 Topology optimization of a pipe bend

In the second test case the pressure drop in a pipe bend is minimized. This problem is a commonly used test case for the investigation of topology optimization methods and was first introduced by Borrvall and Petersson [12]. The geometry of the flow domain is depicted in Figure 4. The grid for this test case consists of  $100 \times 100$  control volumes. For

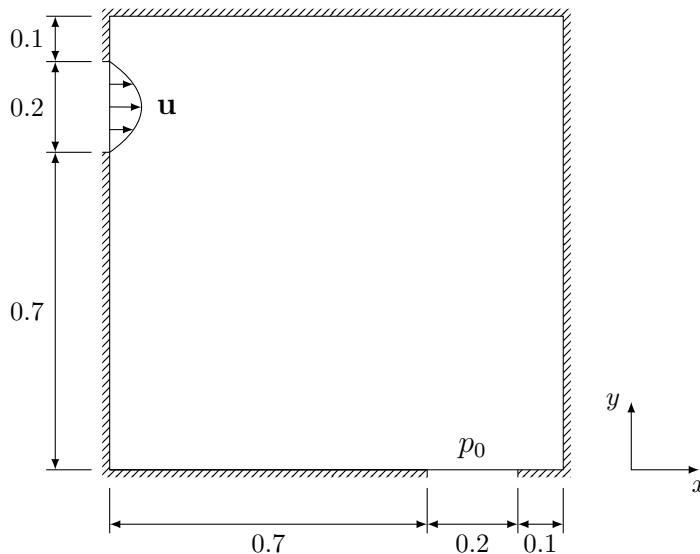


**Figure 4:** Flow domain of the pipe bend test case with inlet and outlet boundary conditions

the inflow a parabolic velocity profile is used and the Reynolds number is set to  $Re = 10$  based on the inlet height. The objective is to minimize the pressure drop between the inlet and the outlet. Thus, the optimization problem is defined as

$$\begin{aligned} \min_{\mathbf{a}} \quad & J = \bar{p}_{in} - \bar{p}_{out}, \\ \text{s. t.} \quad & g = \frac{A_{fluid}}{A_{total}} - 0.25 \leq 0, \end{aligned} \tag{10}$$

where  $\bar{p}_{in}$  is the mean pressure at the inlet and  $\bar{p}_{out}$  is the mean pressure at the outlet. The constraint  $g$  allows only 25% of the flow domain to be fluid. The test case is optimized with three different initial designs. For the first design two NURBS curves are used which

are shown in Figure 5 and are defined by the control points

$$\mathbf{P}_1^1 = \begin{pmatrix} 0.0 \\ 0.7 \end{pmatrix}, \quad \mathbf{P}_2^1 = \begin{pmatrix} 0.0 \\ 0.0 \end{pmatrix}, \quad \mathbf{P}_3^1 = \begin{pmatrix} 0.7 \\ 0.0 \end{pmatrix} \quad (11)$$

and

$$\mathbf{P}_1^2 = \begin{pmatrix} 0.0 \\ 0.9 \end{pmatrix}, \quad \mathbf{P}_2^2 = \begin{pmatrix} 0.9 \\ 0.9 \end{pmatrix}, \quad \mathbf{P}_3^2 = \begin{pmatrix} 0.9 \\ 0.0 \end{pmatrix} \quad (12)$$

and the knot vector  $U = \{0, 0, 0, 1, 1, 1\}$  for each NURBS. Again all weights are set to one. Four design variables  $a_1, \dots, a_4$  are used to move the control points  $\mathbf{P}_2^1$  and  $\mathbf{P}_2^2$  with

$$\mathbf{P}_2^1 = \begin{pmatrix} 0.0 \\ 0.0 \end{pmatrix} + \begin{pmatrix} a_1 \\ a_2 \end{pmatrix}, \quad \mathbf{P}_2^2 = \begin{pmatrix} 0.9 \\ 0.9 \end{pmatrix} + \begin{pmatrix} a_3 \\ a_4 \end{pmatrix} \quad (13)$$

while the other control points stay fixed. Thus, this case is comparable to the diffuser test case in terms of the NURBS description and can be referred to as a shape optimization.

For the other two initial designs of the test case closed NURBS curves are used. Each of them is defined by six control points as shown in Figure 6. To ensure a smooth closed

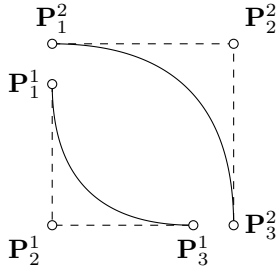


**Figure 5:** Open NURBS curves each defined by three control points

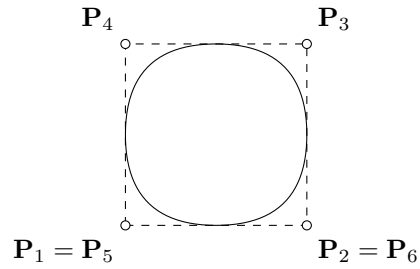


**Figure 6:** Closed NURBS curve defined by six control points

curve the first two control points are repeated according to the degree of the curves. All of these curves are defined relative to their center by

$$\mathbf{P}_1 = \mathbf{P}_5 = \begin{pmatrix} -0.1 \\ -0.1 \end{pmatrix}, \quad \mathbf{P}_2 = \mathbf{P}_6 = \begin{pmatrix} 0.1 \\ -0.1 \end{pmatrix}, \quad \mathbf{P}_3 = \begin{pmatrix} 0.1 \\ 0.1 \end{pmatrix}, \quad \mathbf{P}_4 = \begin{pmatrix} -0.1 \\ 0.1 \end{pmatrix} \quad (14)$$

with the unclamped, uniform knot vector  $U = \{0, \dots, 8\}$ . Again all weights are set to one and each coordinate is controlled by a separate design variable. At first two of these closed curves are used with the centers  $(0.3, 0.3)$  and  $(0.7, 0.7)$ . The last case uses four curves with the centers  $(0.25, 0.50)$ ,  $(0.50, 0.75)$ ,  $(0.75, 0.50)$  and  $(0.50, 0.25)$ .

The results are shown in Figure 7 including the streamlines for the initial and the optimized design. All of the three initial designs lead to very similar results as well for the value of the objective function as for the immersed boundaries. To reach the final design a topological change of the flow domain had to happen for the second and the third variant which proves the capability of the proposed method for topology optimization.

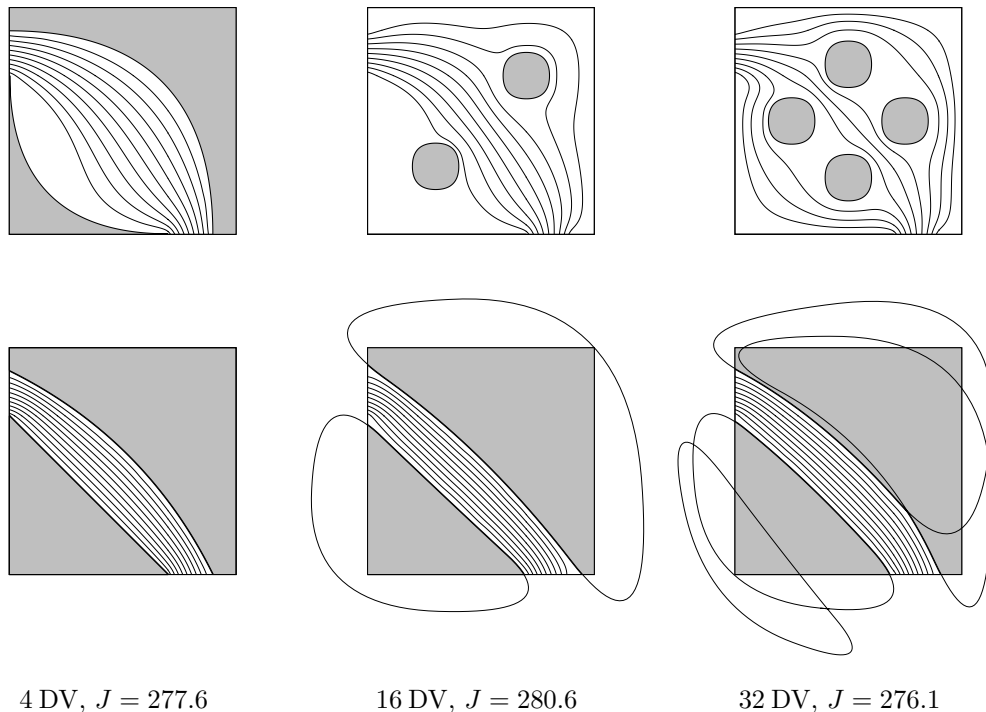


**Figure 7:** Results for the pipe bend test case with different initial designs and different number of design variables (DV), showing the corresponding NURBS curves and the streamlines

The third variant also shows the possibility of overlapping NURBS curves, which is a necessary feature to achieve topological changes during the optimization process. The optimized designs shown in Figure 8 are comparable to results from other authors like [12, 13]. The optimization process shows a robust behavior for all test cases and a fast convergence as shown in Figure 9. The peak at the beginning of each optimization results from the fact that the volume constraint is violated at start. Therefore, the optimization algorithm first tries to satisfy the constraint before minimizing the pressure drop. For 4 design variables the stopping criteria is already reached after 11 iterations. For 16 and 32 design variables the optimum is reached after 175 and 94 iterations, respectively. However, it can be seen that a value near the optimum is already reached much earlier. For 16 and 32 design variables the objective function drops below 300 after about 30 iterations. Also no oscillations of the objective function value during the optimization process could be observed as reported by other authors [3].

## 5 CONCLUSION

A NURBS-based framework for shape and topology optimization was presented. The Brinkman penalization method was used to account for solid areas in the flow domain. The solid boundaries were mathematically described by NURBS curves. To determine the Brinkman penalization parameter in each control volume the Sutherland-Hodgman algorithm was used. The proposed method was investigated with two test cases to prove

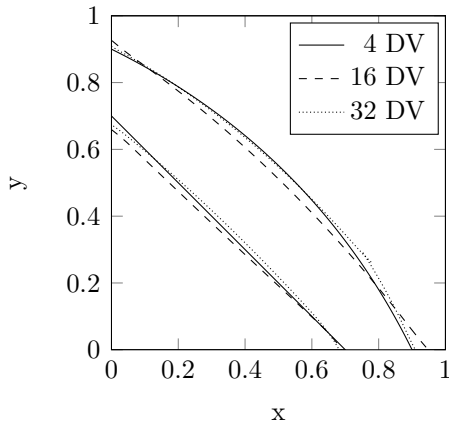


**Figure 8:** Final immersed boundaries for the different initial designs of the pipe bend test case

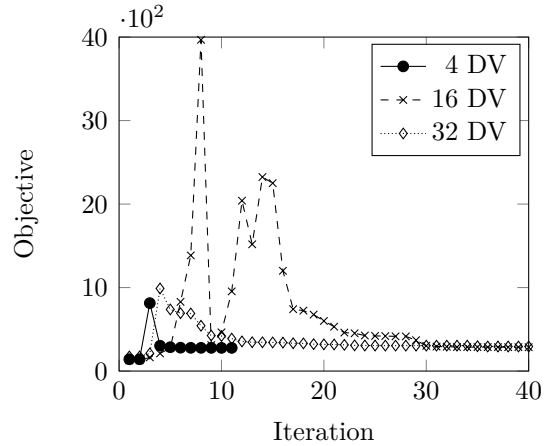


**Figure 9:** Convergence for the different initial designs of the pipe bend test case

the capability for shape and topology optimization. The results show a high potential in both disciplines. The method showed a fast and robust convergence for the optimization process and can lead to complex designs with a small number of design variables compared to traditional topology optimization approaches. The next steps will be the extension of the framework to three-dimensional problems as well as the calculation of the gradient with a direct approach.

## REFERENCES

- [1] Bendsøe, M.P. and Sigmund, O. Topology optimization: theory, methods, and applications. *Springer Science & Business Media* (2003).
- [2] Sigmund, O. and Maute, K. Topology optimization approaches. *Structural and Multidisciplinary Optimization* (2013) **48**(6):1031-1055.
- [3] Pingen, G., Waidmann, M., Evgrafov, A. and Maute, K. A parametric level-set approach for topology optimization of flow domains. *Structural and Multidisciplinary Optimization* (2010) **41**(1):117-131.
- [4] Angot, P., Bruneau, C.-H. and Fabrie, P. A penalization method to take into account obstacles in incompressible viscous flows. *Numerische Mathematik* (1999) **81**(4):497-520.
- [5] Kreissl, S., Pingen, G. and Maute, K. Topology optimization for unsteady flow. *International Journal for Numerical Methods in Engineering* (2011) **87**(13):1229-1253.
- [6] De Boor, C. A practical guide to splines. *New York: Springer-Verlag* (1978).
- [7] Piegl, L. and Tiller, W. The NURBS book. *Springer Science & Business Media* (1997).

- [8] Sutherland, I.E. and Hodgman, G.W. Reentrant polygon clipping. *Communications of the ACM* (1974) **17**(1):32-42.
- [9] Durst, F. and Schäfer, M. A Parallel Block-Structured Multigrid Method for the Prediction of Incompressible Flows. *International Journal for Numerical Methods in Fluids* (1996) **22**(6):549-565.
- [10] Svanberg, K. A globally convergent version of MMA without linesearch. In *Proceedings of the First World Congress of Structural and Multidisciplinary Optimization*, N. Olhoff and G. Rozvany, eds., Pergamon Press, Elmsford, NY (1995) 9-16.
- [11] Michaelis, J. Parallele Mehrgitter-Strategien zur Sensitivitätsanalyse und Strömungsoptimierung. *Dr. Hut* (2013).
- [12] Borrvall, T. and Petersson, J. Topology Optimization of Fluids in Stokes Flow. *International Journal for Numerical Methods in Fluids* (2003) **41**:77-107.
- [13] Pingen, G., Evgrafov, A. and Maute, K. Topology Optimization of Flow Domains Using the Lattice Boltzmann Method. *Structural and Multidisciplinary Optimization* (2007) **34**(6):507-524.